

Interactions between climate change, urban infrastructure and mobility are driving dengue emergence in Vietnam

Rory Gibb¹⁻⁴, Felipe J. Colón-González^{1-3,5}, Phan Trong Lan⁶, Phan Thi Huong⁶, Vu Sinh Nam⁷, Vu Trong Duoc⁷, Do Thai Hung⁸, Nguyễn Thanh Dong⁸, Vien Chinh Chien⁹, Ly Thi Thuy Trang⁹, Do Kien Quoc¹⁰, Tran Minh Hoa¹¹, Nguyen Hữu Tai¹², Tran Thi Hang¹³, Gina Tsarouchi¹⁴, Eleanor Ainscoe¹⁴, Quillon Harpham¹⁴, Barbara Hofmann¹⁴, Darren Lumbroso¹⁴, Oliver J. Brady^{*1,2}, Rachel Lowe^{*1-3,15,16}

¹Centre for Mathematical Modelling of Infectious Diseases, London School of Hygiene and Tropical Medicine, UK.

²Department of Infectious Disease Epidemiology, Faculty of Epidemiology and Population Health, London School of Hygiene & Tropical Medicine, London, UK

³Centre on Climate Change and Planetary Health, London School of Hygiene and Tropical Medicine, UK.

⁴Centre for Biodiversity and Environment Research, Department of Genetics, Evolution & Environment, University College London, UK.

⁵Data for Science and Health, Wellcome Trust, London, UK.

⁶General Department of Preventative Medicine (GDPM), Ministry of Health, Vietnam.

⁷National Institute of Hygiene and Epidemiology (NIHE), Hanoi, Vietnam.

⁸Pasteur Institute Nha Trang, Nha Trang, Khanh Hoa Province, Vietnam.

⁹Tay Nguyen Institute of Hygiene and Epidemiology (TIHE), Buon Ma Thuot, Dak Lak Province, Vietnam.

¹⁰Pasteur Institute Ho Chi Minh City, Ho Chi Minh City, Vietnam.

¹¹Center for Disease Control, Dong Nai Province, Vietnam.

¹²Center for Disease Control, Khanh Hoa Province, Vietnam.

¹³Center for Disease Control, Hanoi, Vietnam.

¹⁴HR Wallingford, Wallingford, Oxfordshire, UK.

¹⁵Barcelona Supercomputing Center (BSC), Barcelona, Spain.

¹⁶Catalan Institution for Research and Advanced Studies (ICREA), Barcelona, Spain.

Correspondence to Rory Gibb (rory.gibb.14@ucl.ac.uk)

* Denotes equal author contributions

42 Abstract

43 Dengue is expanding globally, but how dengue emergence is shaped locally by interactions
44 between climatic and socio-environmental factors is not well understood. Here, we investigate
45 the drivers of dengue incidence and emergence in Vietnam, through analyzing 23-years of
46 monthly district-level case data spanning a period of significant socioeconomic change (1998-
47 2020). We show that urban infrastructure factors (sanitation, water supply and long-term urban
48 growth) predict local spatial patterns of dengue incidence, while human mobility is a more
49 influential driver in subtropical northern regions than the endemic south. Temperature is the
50 dominant factor shaping dengue's geographical distribution and dynamics, and using long-term
51 reanalysis temperature data we show that recent warming (since 1950) has generally expanded
52 transmission risk throughout Vietnam, and most strongly in current dengue emergence hotspots
53 (e.g. southern central regions and Ha Noi). In contrast, effects of hydrometeorology are complex,
54 multi-scalar and dependent on local context: risk increases under both short-term precipitation
55 excess and long-term drought, but improvements in water supply largely mitigate drought-
56 associated risks except under extreme conditions. Our findings challenge the assumption that
57 dengue is an urban disease, instead suggesting that incidence peaks in transitional landscapes
58 with intermediate infrastructure provision, and provide evidence that interactions between recent
59 climate change and mobility have contributed to dengue's ongoing expansion throughout
60 Vietnam.

61 Introduction

62 Socio-environmental and climatic changes are reshaping the dynamics and distributions of
63 infectious diseases worldwide, with urgent consequences for public health¹⁻³. In recent decades
64 these impacts have been especially pronounced for *Aedes* mosquito-borne arboviral infections
65 (e.g. dengue, chikungunya and Zika), whose vectors are specialised for life in the emerging
66 urbanised landscapes of the 21st century⁴. Dengue is an acute febrile illness caused by any one
67 of four major dengue virus (DENV) serotypes and is principally transmitted by *Ae. aegypti*, a
68 human-specialist that breeds using water-related features of built environments (e.g. water
69 containers in homes, gutters, drains and sewerage systems)^{5,6}. The burden of dengue is rapidly
70 growing, with incidence doubling each decade since 1990⁷, cases reported from more than 125
71 countries⁸, and extremely widespread outbreaks increasing in frequency⁵. The disease is also
72 expanding geographically into more remote regions^{9,10}, and to higher latitudes^{11,12} and altitudes¹³
73 at the margins of its historical range. These emergence trends are broadly thought to be driven
74 by increasing human mobility^{14,15}, expansion of anthropogenic and semi-urbanised landscapes¹⁰
75 and changing climatic suitability¹⁶, and have complicated the historical perception of dengue as
76 mainly a disease of major tropical cities¹⁷. Cities are important regional foci of dengue burden
77 and DENV diversity in endemic areas, with human host densities typically high enough to support
78 sustained transmission¹⁸⁻²⁰. However, more local patterns of transmission are often highly
79 variable, and shaped by both built environment characteristics that influence vector populations
80 and behaviour²¹ (e.g. housing quality, drainage, heat islands), and human movement patterns
81 that drive viral dispersal between locations^{22,23}. Together these processes produce
82 heterogeneous patterns of disease²¹, for example between neighbourhoods²⁴ or between major
83 metropolises and smaller cities¹⁴. Yet it remains unclear which socio-environmental features are

84 most influential in driving this local variability in dengue risk across wide geographical areas.
85 Importantly, it is also unclear how recent and ongoing climatic and socio-environmental changes
86 – such as warming, urbanisation and mobility growth in many endemic countries – may be
87 interacting to reshape the disease’s distribution.

88 Dengue is commonly associated with urban habitats²⁵, which provide both high densities of
89 *Aedes* breeding habitat and amenable microclimates^{6,26}. Urban growth is often cited as a key
90 driver, but the extent to which this influences dengue transmission probably depends on the
91 timescale and characteristics of the urbanisation process. For example, expansion of built
92 environments in the short-term may create many temporary open mosquito breeding habitats
93 during the construction phase, and informal settlements (where infrastructure and services
94 provision lag behind growth) may be more likely to increase risk compared to longer-term
95 planned urban development. The link between dengue risk and water supply and sanitation
96 infrastructure remains poorly understood, but these may be important factors determining
97 spatial heterogeneity in transmission. Access to the piped water network should reduce
98 households’ need to store water in containers, and in household-level studies piped water access
99 is often (but not always) associated with lower dengue risk²⁷⁻²⁹. Improvements in sanitation
100 systems might similarly reduce risk by reducing the density of water storage containers;
101 however, if not well-maintained, drains and septic tanks can be productive mosquito breeding
102 sites³⁰. Alternatively, human mobility patterns – which drive viral dispersal at multiple scales –
103 might be the dominant spatial driver of dengue. Well-connected hubs in international transport
104 networks (e.g. metropolises or regional capitals) often experience high rates of long-range DENV
105 strain importation, seeding transmission chains that spread among closely-linked areas via local
106 traffic (e.g. commuter flows)^{15,20,31}. Higher mobility might therefore be particularly important to
107 maintenance of dengue transmission in areas where epidemic fade-outs are more likely³², such
108 as with lower population densities or seasonally-transient climatic suitability.

109 Climate has strong impacts on biophysical suitability for vector populations and dengue
110 transmission. Air and water temperature affect numerous biological processes in mosquitoes
111 that regulate population dynamics and vector competence (e.g. growth, survival, reproductive
112 rate, extrinsic incubation period), which combined predict a nonlinear relationship between
113 temperature and transmission intensity²⁶. Temperature variability can underpin dengue outbreak
114 seasonality³¹ and transmission season length³³, and future warming temperatures are projected
115 to significantly expand dengue transmission suitability worldwide³⁴. However, there remains little
116 evidence for how warming to date may have shaped recent dengue distribution and expansion
117 trends. Precipitation patterns drive the creation and flushing of vector breeding sites³⁵, but their
118 relationship to dengue transmission may often be nonlinear, delayed, and determined by how
119 seasonality and extremes interact with local socio-environmental factors. For example, in Brazil
120 and Barbados dengue risk sharply increases several months after periods of drought³⁶,
121 particularly in urban areas with unreliable water supply³⁷, suggesting a mediating role of water
122 storage behaviour in response to rainfall shortages. These recent studies imply that local dengue
123 responses to climatic drivers might differ markedly between neighbouring areas with different
124 socioeconomic characteristics^{21,38}. Further understanding such cross-scale interactions might
125 improve the predictability of spatial outbreak dynamics in response to large-scale
126 hydrometeorological phenomena such as droughts.

127 In this study, we investigate these interacting effects of climatic and socio-environmental drivers
128 on dengue incidence and emergence in Vietnam, by analysing 23 years (1998-2020) of monthly
129 district-level (2nd administrative level) case surveillance data. Dengue is a major public health
130 issue in Vietnam, which typically records among the highest incidence rates in Southeast Asia³⁹,
131 although with wide variation in transmission intensity across the country's broad latitudinal and
132 altitudinal range⁴⁰. The south has a tropical monsoon climate and experiences fairly stable,
133 seasonal endemic dynamics^{40,41}. In the subtropical north, winter temperatures are too cool to
134 support transmission⁴²⁻⁴⁴ so dengue occurs in sporadic outbreaks during warmer months (often
135 seeded by DENV reintroductions from the south⁴²). In recent decades, Vietnam has undergone a
136 major economic transformation from low-income towards middle-income, and has seen rapid
137 development of major and regional cities, sharply rising population mobility via road and air
138 (from ~3 million to ~53 million air passengers carried between 2000-2019⁴⁵), and expansion of
139 access to hygienic water supply and sanitation infrastructure to much of the population⁴⁶. During
140 the same period the country has also experienced warming temperatures and more frequent
141 extreme weather events such as heatwaves and drought, and is considered particularly
142 vulnerable to health impacts of climate change⁴⁷. Currently there is still little empirical evidence
143 for how interactions between such rapid socioeconomic and climatic changes may impact the
144 distribution and burden of dengue, making Vietnam an ideal historical setting to ask this
145 question. We used Bayesian hierarchical models and block cross-validation experiments to infer
146 relationships between socio-environmental and climatic covariates and dengue risk (Table 1),
147 and explore their effects on spatiotemporal patterns of incidence. We aimed to answer two main
148 questions. Firstly, what are the most influential spatial and temporal drivers of dengue incidence
149 across Vietnam, and how might these have contributed to recent dengue trends? Secondly, how
150 does local urban infrastructure affect the relationship between hydrometeorological dynamics
151 and dengue incidence?

152 **Results**

153 **Surveillance data show a recent expansion of dengue incidence across much of Vietnam**

154 Vietnam is administratively divided into 58 provinces and 5 major urban municipalities including
155 its two main economic centres, Ha Noi and Ho Chi Minh City (Figure 1). Since 1999 the country
156 has maintained a national dengue passive surveillance system, with monthly reported case
157 counts recorded at district-level (administrative level-2) (Methods, Supp. Figure 1). Dengue
158 incidence typically peaks between June and November (Supp. Figure 1), so our analyses defined
159 transmission years as running from May to April. The surveillance dataset included 174,936
160 monthly case counts totalling 2,038,380 dengue cases identified via passive surveillance (either
161 clinically suspected or laboratory confirmed), from 667 districts between May 1998 and April
162 2021 (Methods). The highest country-wide counts were in 2019 (294,707) and 2018 (170,600),
163 and the lowest in 2014 (34,258) and 2002 (35,386). Surveillance data show regional differences
164 in transmission settings, with the south experiencing endemic dynamics, and the north sporadic
165 outbreaks mainly restricted to Ha Noi and the Red River Delta (Figure 1a, Supp. Figure 1). Large
166 synchronous outbreaks occurred nationally in 1998, 2010, 2017 (mainly in the north) and 2019
167 (mainly central and south) (Supp. Figure 1). We mapped directional trends in dengue incidence at
168 district-level by estimating the slopes of annual log incidence using linear regression (Figure 1b).
169 This shows strong evidence ($p < 0.01$) of upward trends throughout the southern central regions

170 (South Central Coast, Central Highlands; up to a 45% year-on-year increase in some districts),
171 Red River Delta, and parts of the Southeast (Figure 1b). The pronounced geographical pattern
172 and absence of obvious step changes in case numbers suggest that these trends are unlikely to
173 be solely driven by specific changes in surveillance or diagnostic practices, and therefore are
174 likely to reflect a true expansion.

175 **National and regional trends in urbanization, infrastructure, mobility and climate**

176 We derived district-level covariates to represent key hypothesized drivers, from census sources,
177 remote sensing data⁴⁸, human mobility models and climate reanalysis (ERA5-Land temperature
178 and bias-corrected ERA5 precipitation^{49,50}; Table 1, Methods, Supp. Text 1). These included:
179 annual population density; socio-environmental features (built-up land extent, short-term and
180 long-term urban expansion rates, improved water access, hygienic toilet access, per-capita road
181 travel rates, mobility flux predicted from naïve gravity and radiation models); annual temperature
182 metrics to represent thermal constraints on dengue persistence (mean and minimum); and
183 monthly means of air temperature (T_{\min} , T_{mean} and T_{\max}), precipitation, and multi-scalar drought
184 indicators (Standardized Precipitation Evapotranspiration Index, SPEI⁵¹, in 1-, 6-, and 12-month
185 time windows) at lags of 0 to 6 months. SPEI measures accumulated hydrological surplus or
186 deficit relative to the long-term historical average for the same period of the year^{52,53}. Its multi-
187 scalar nature enables measurement of hydrometeorological dynamics at timescales ranging
188 from transient (affecting surface water) to long-term (affecting reservoir and groundwater
189 levels), and thus different potential causal influences on dengue transmission (Table 1).
190 Covariates and hypothesized relationships are summarized in Table 1, with data sources and
191 processing described in Methods and Supp. Text 1.

192 The study period saw nationwide upward trends in urbanization, mobility and infrastructure
193 improvement, although with regional variation (Figure 2, Supp. Figure 2). Urban extent and urban
194 growth, population density, mobility, and improved water and sanitation access are generally
195 highest in the regions containing Vietnam's largest economic centres, Southeast (Ho Chi Minh
196 City) and Red River Delta (Ha Noi). Per-capita road traffic rates (reported annually at province-
197 level⁵⁴) increased rapidly nationwide between 1998 and 2019 – ranging from 4.5-fold growth in
198 the Mekong River Delta and Northwest to 14-fold in the Red River Delta – and declined in 2020
199 reflecting COVID-19 associated movement restrictions. Census estimates also showed a
200 nationwide expansion in the proportion of households reporting access to improved water
201 supply (piped or borehole-derived water) and hygienic toilet facilities (indoor/outdoor flush toilet;
202 this rose sharply from 2009-2019). Temperature becomes cooler and more seasonally variable
203 along the south-to-north gradient, while precipitation is generally highest and most variable in the
204 central regions (Figure 2, Supp. Figures 2-4). Hydrometeorological extremes at short timescales
205 (SPEI-1) are relatively variable among neighbouring districts (i.e. at small spatial scales),
206 whereas at longer timescales (SPEI-6) they tend to be more spatially synchronised at the
207 regional level (Supp. Figure 3).

208 **Urban infrastructure, temperature and hydrometeorology are important spatial and seasonal 209 drivers of dengue incidence**

210 We fitted Bayesian spatiotemporal regression models to the surveillance dataset, with monthly
211 case counts modelled using a negative binomial likelihood (Methods). Seasonality was

212 represented with a province-specific temporally-correlated effect of calendar month (*'seasonal*
213 *random effect'*). Unexplained spatiotemporal variation, for example due to immunity and DENV
214 serotype dynamics or changing surveillance sensitivity, was accounted for with dengue year-
215 specific district-level spatially-structured and unstructured effects⁵⁵ (*'district-level random*
216 *effects'*). A random effects-only (*'baseline'*) model captured declines in dengue relative risk (RR)
217 and greater seasonal variability with increasing latitude (Supp. Figure 5). We then tested whether
218 socio-environmental covariates (specified as either linear, logarithmic or nonlinear terms) and
219 monthly climate variables (at lags from 0 to 6 months) improved model adequacy metrics and
220 reduced unexplained variation in district-level random effects, compared to the baseline
221 (Methods, Supp. Figure 6). There were greater improvements from including gravity rather than
222 radiation model-based mobility flux; long-term urban expansion (in the preceding 10-year
223 window) rather than short-term (3-year window); SPEI metrics rather than precipitation; and T_{mean}
224 of the coolest month rather than other annual temperature metrics (Supp. Figures 6-7).

225 We developed a full multivariate model (Figure 3, Methods) including fixed effects of T_{mean}
226 coolest month, built-up land cover, 10-year urban expansion rate (log), gravity flux (log) and road
227 travel per inhabitant (log), and nonlinear effects of hygienic toilet access, improved water access
228 and monthly T_{mean} (1-month lag), SPEI-1 (1-month lag) and SPEI-6 (5-month lag). The full model
229 substantially improved all information criteria (Supp. Table 2-3). Structured predictive
230 experiments can provide insights into the generality of drivers, through identifying variables that
231 improve predictive accuracy in unobserved locations and times^{56,57}. To estimate the individual
232 predictive influence of each covariate, we used 5-fold cross-validation to estimate model
233 prediction error (out of sample mean absolute error, MAE_{OOS}) under 3 block holdout designs, in
234 turn excluding one covariate at a time from the full model (Methods, Supp. Figure 8). We defined
235 a variable's 'predictive influence' as the change in MAE_{OOS} when it is excluded (Figure 4). We
236 measured covariates' influence on predicting spatial heterogeneity in incidence using 'spatial'
237 and 'spatiotemporal' block designs (5-fold blocked by district and district-year respectively), and
238 on predicting temporal dynamics using 'seasonal' block design (5-fold by district-quarter;
239 monthly climate variables only) (Supp. Figure 8). The full model significantly reduced prediction
240 error compared to the baseline under all block designs (Figure 4, Supp. Figure 9).

241 The most influential local spatial drivers of dengue risk related to infrastructure and urban
242 expansion, followed by temperature and SPEI-1 (Figure 4a-b). Increasing access to hygienic
243 toilets had a positive marginal relationship with dengue risk (Figure 3c) with the highest
244 predictive influence (Figure 4a-b). The effect of population access to improved water supply was
245 nonlinear, with risk peaking at a low-to-intermediate level (around 25% of households) and
246 declining thereafter (Figure 3d). Urbanization metrics had generally protective effects, with a
247 strongly negative relationship between dengue risk and long-term urban expansion (in the
248 preceding 10 years) with a high predictive influence (Figure 3b, Figure 4a-b), and a weaker
249 negative effect of built-up land cover. Mobility metrics (per-capita road traffic rates and gravity
250 flux) had positive relationships with dengue risk (Figure 3b) but little overall predictive influence
251 (Figure 4). All inferred socio-environmental effects were robust to sensitivity analysis by census-
252 defined level of urbanization (Supp. Figure 10).

253 Overall, there was strong evidence that temperature is a dominant factor shaping both the broad
254 geographical distribution and temporal dynamics of dengue incidence across Vietnam. Annual
255 T_{mean} of the coolest month had a large positive effect on dengue risk and contributed
256 significantly to spatial prediction (Figure 3a, Figure 4a-b), probably through impacting vector
257 survival during the least thermally-suitable period of the year. Notably, including this covariate
258 alone reduced unexplained variation in the district-level random effects by 50%, providing strong
259 evidence that thermal constraints on year-round DENV transmission by mosquitoes are a key
260 determinant of the geographical gradient of dengue across Vietnam (Supp. Figure 7). Monthly
261 mean temperature (T_{mean}) had a nonlinear and delayed (1-month lag) effect, with relative risk
262 increasing to a peak around 27°C and declining sharply at higher temperatures, consistent with
263 expectations based on dengue's thermal biology²⁶. Monthly T_{mean} contributed significantly to
264 spatial prediction (Figure 4a-b) and was the main predictor of temporal dynamics (Figure 4c).

265 Hydrometeorological dynamics had delayed and nonlinear effects that depended on timescale:
266 increases in relative risk were associated with transient excess wet conditions at short lead
267 times (SPEI-1 1 month lag), and with long-term accumulated drought at longer lead times (SPEI-6
268 5-month lag) (Figure 3f-g). SPEI-1 had a positive predictive influence on both spatial and
269 temporal dengue dynamics (Figure 4). In contrast, SPEI-6 did not substantially contribute to
270 spatial prediction (Figure 4a-b) despite improving temporal predictions (Figure 4c). It is possible
271 that the regional synchrony of long-term drought (Supp. Figure 3) makes it less predictive of
272 finer-scale spatial heterogeneity in dengue incidence, in the absence of information about local
273 mediating socio-environmental features.

274 **The importance of human mobility is greater in northern Vietnam where dengue is emerging**

275 The importance of drivers might vary between endemic contexts (i.e. where dengue persists
276 year-round) and emerging settings, where sustained transmission is constrained by factors such
277 as remoteness or transient climatic suitability. We examined this by fitting separate models for
278 Vietnam's southern (Mekong River Delta, Southeast, South Central Coast and Central Highlands)
279 and northern regions (North Central, Red River Delta, Northeast, Northwest), which broadly
280 delineate areas of endemic and sporadic transmission (Figure 1, Supp. Figure 1, Supp. Figure 5).
281 The inferred shape and directionality of socio-environmental effects were very similar between
282 regions, albeit with generally larger fixed effects slope estimates in the north, reflecting the lower
283 incidence of dengue compared to the national average (Supp. Figure 11). The major notable
284 difference is that mobility variables (per-capita road traffic rates and gravity flux) have relatively
285 much larger positive effects on dengue incidence in northern Vietnam than in the endemic south
286 (Supp. Figure 11). The same regional differences are reflected in covariates' relative predictive
287 influence under block cross-validation: the top-ranked spatial predictors in the north are mobility
288 and temperature variables, compared to infrastructure, temperature and urbanization in the
289 south (Supp. Figure 12).

290 **Climate change is reshaping the geography of dengue transmission across Vietnam**

291 Ongoing climatic changes might be contributing to recent dengue emergence trends, particularly
292 in the central and northern regions of Vietnam (Figure 1b). To investigate this, we tested for
293 significant changes in monthly temperature-driven dengue risk between a historical reference
294 period (1951-1970) and the present-day (2001-2020) using long-term ERA5-Land reanalysis

295 data⁵⁸ (Methods). We used the inferred risk function for T_{mean} (Figure 3e) to predict monthly
296 posterior marginal mean temperature-driven risk since 1950 (i.e. just the effect of temperature
297 while holding all other variables constant), then used linear models to test for differences
298 between reference and present day periods, comparing 20-year averages to account for natural
299 climate system variability (Methods, Figure 5). Present-day projections of temperature-driven risk
300 (Figure 5) reproduce the gradient of observed transmission, with high risk year-round in the
301 south, and seasonally transient risk in the north that declines during winter months (January to
302 April; Figure 5a).

303 Increasing temperatures since the 1951-1970 reference period have driven expansion and
304 redistribution of predicted dengue risk across much of Vietnam (Figure 5b-c, Supp. Figures 13-
305 14). Predicted risk increases are particularly pronounced in southern central regions, including
306 during low-season months in the higher-altitude Central Highlands provinces (up to 56%
307 increase), suggesting that climate change is expanding the suitable area for endemic
308 transmission. Similarly, much of north Vietnam has experienced sharp rises in risk during
309 summer months, including in more remote northern regions, and a lengthening of the
310 transmission season in the Red River Delta including Ha Noi (Figure 5b-c). Notably, these
311 hotspots of increasing temperature-driven risk are geographically concordant with the steepest
312 upward dengue trends during the 1998-2020 period (Figure 1b) and with visual indications of a
313 transition from sporadic outbreaks towards endemic transmission in southern central regions
314 (Supp. Figure 1). Overall, these results suggest that recent warming has reduced thermal
315 constraints on dengue transmission in much of Vietnam and probably contributed to recent
316 northward and altitudinal shifts. Notably, however, there is also evidence of seasonal and spatial
317 redistribution of transmission, with rising temperatures above dengue's thermal optimum slightly
318 reducing risk during the hottest months of the year in parts of the south (April-July) and north
319 and coastal areas (July-August), compared to the historical reference period (Figure 4b-c, Supp.
320 Figures 13-14). Far fewer climate observations are assimilated by ERA5 during earlier years (up
321 to the late 1960s), which may impact the accuracy of reanalysis estimates⁵⁸; as a sensitivity test
322 we therefore repeated this analysis using a later reference period (1971-1990), which showed
323 very similar overall results (Supp. Figure 15).

324 **The effects of hydrometeorology on dengue incidence are multi-scalar and modified by local** 325 **infrastructure**

326 Theory and recent empirical evidence suggest that local socio-environmental context may be
327 important in determining dengue's response to precipitation and drought patterns^{35,37}. We
328 investigated the multi-scalar effects of hydrometeorological dynamics on dengue incidence,
329 focusing on southern Vietnam where transmission occurs year-round (Methods). We found
330 evidence of delayed and timescale-dependent relationships between hydrometeorology and
331 dengue risk: the increase in risk driven by transient wet conditions (SPEI-1) peaks at a 1 to 2
332 month delay and declines sharply beyond 2 months, whereas risk associated with long-timescale
333 drought (SPEI-6) emerges gradually over a longer delay period (from 4 to 6 months) (Supp.
334 Figure 16). This suggests that hydrometeorological phenomena at different timescales probably
335 affect dengue risk via different causal pathways, one mainly biophysical (high rainfall leading to
336 immediate proliferation of outdoor vector breeding sites) and the other behavioural (household
337 water storage in response to perceived sustained shortages).

338 If the long-term drought effect is mainly mediated by water storage behaviour, we hypothesized
339 that increasing population access to improved water supply (i.e. more reliable than rainwater⁵⁹)
340 would reduce the dengue risks associated with sustained drought but not with short-term excess
341 (Methods). We also expected that, at this fine spatial scale, including an interaction with water
342 supply would explain observed patterns better than an interaction with urbanisation (which was
343 found to significantly modify drought effects in a recent coarser-scale study³⁷). We tested this by
344 stratifying the effects of either SPEI-1 (1-month lag) or SPEI-6 (5-month lag) by low (<25%),
345 intermediate (25-75%) and high (>75%) levels of either water supply (proportion of households)
346 or built-up land cover, within the full model retaining all other covariates (Methods). Consistent
347 with our expectations, models including an interaction between SPEI-6 and water supply
348 substantially improved model fit, whereas interactions with urban land and with SPEI-1 did not
349 improve models (Supp. Figure 17-18). The interaction model showed a complex, nonlinear
350 relationship between sustained drought, improved water supply and dengue risk (Figure 6a).
351 Increasing access to improved water supply reduces the delayed dengue risk associated with
352 near normal to moderately dry conditions (SPEI-6 between 0 and -1.5), but sharply increases the
353 risk under moderate to extreme drought conditions (SPEI-6 < -1.5). In contrast, where improved
354 water supply is low, increasingly dry conditions are associated with linear increases in risk
355 except during rare periods of severe drought, when risk slightly declines (SPEI-6 < -2, 1.5% of
356 observations). Long-term wet conditions (SPEI-6 > 0) are protective across all strata (Figure 5a).
357 Notably, including this interaction substantially reduced prediction error under spatiotemporal
358 and seasonal holdout designs compared to a non-interaction model (Supp. Figure 18), providing
359 evidence that accounting for cross-scale climatic and socio-environmental interactions can help
360 to predict spatial variation in dengue risk.

361 To visualise how interactions between drought and improved water supply could produce spatial
362 heterogeneity in dengue dynamics, we projected monthly SPEI-6 associated relative risk for an
363 example time series from the Mekong River Delta (2002-2020), under scenarios of low,
364 intermediate and high water supply (Figure 6b). Over two decades, SPEI-6 oscillates between
365 periods of near normal to moderately dry and wet, with rarer extremes (droughts in 2003-4 and
366 2016-17, excess in 2018-19; Figure 6b, top panel). Under low-to-intermediate improved water
367 supply (<75% of households), dengue relative risk is closely linked to these oscillations,
368 significantly increasing during regular dry periods. In contrast, when improved water supply is
369 high (>75%) risk is effectively dampened during these lower amplitude dry periods, instead only
370 increasing sharply during sporadic periods of severe drought (Figure 6b, bottom panel).

371 Discussion

372 Despite recognition of the growing threat of dengue under global change⁵, understanding of how
373 key socio-environmental and climatic drivers shape both local patterns of transmission and
374 broader emergence trends remains patchy. By analysing 23-years of dengue surveillance data
375 across a gradient of transmission intensity in Vietnam, we found that urban infrastructure-related
376 metrics (water supply, sanitation and long-term urban growth) are the most influential predictors
377 of local heterogeneity in incidence (Figures 3-4). Notably, temperature is a key driver of the
378 distribution and dynamics of dengue, and long-term reanalysis data indicates that recent climate
379 change has already expanded temperature-driven dengue risk across Vietnam (Figure 5). In

380 contrast, effects of hydrometeorology depend on timescale and socioeconomic context, with
381 drought effects mediated by access to improved water supply (Figure 6). These socio-
382 environmental findings complement existing household- and subregional-level evidence for
383 dengue risk factors in Vietnam^{29,40,41,60}, with the benefit that the dataset's long-term nature,
384 spatial granularity and national coverage allowed for inference across the full range of many
385 hypothesized drivers – from rural to urban, remote to highly-connected, and tropical to cooler
386 subtropical climates.

387 **Decomposing the roles of urbanization and infrastructure as spatial drivers of dengue** 388 **incidence**

389 The coarser surveillance data commonly used in large-scale dengue analyses makes it difficult
390 to disentangle the effects of local socio-environmental factors from closely correlated metrics
391 such as population density. Our study at finer scale avoids this issue, and provides evidence that
392 water and sanitation infrastructure are more important spatial determinants of dengue risk than
393 availability of urban habitat *per se*. Increasing hygienic toilet access was the strongest positive
394 predictor, which was unexpected as sanitation improvements are thought to decrease
395 household-level risk. One non-mechanistic explanation is that this metric may index “urban-like”
396 water-related infrastructure that provide amenable *Aedes* breeding habitat, such as storm drains,
397 septic and water storage tanks (although this relationship was robust in a model fitted only to
398 data from rural districts; Supp. Figure 10). Alternatively, increasing flush toilet access could itself
399 drive population-level risk: indoor flush toilets in Vietnam are conventionally linked to septic
400 tanks with storm drain overflows⁴⁶, and outdoor latrines often contain stored water containers,
401 both of which provide vector breeding sites³⁰. Indeed, previous studies in Vietnam have identified
402 outdoor latrine access⁴¹ and proximity to sewage discharge sites⁶¹ as significant household-level
403 risk factors for DENV exposure; our results suggest these effects might be more general, and
404 highlight the need for further research to understand the role of changing sanitation systems in
405 dengue emergence. We also found evidence for protective effects of high improved water supply
406 coverage in both south and north Vietnam, even though our metric was coarse (including both
407 piped and groundwater-derived sources) due to limitations of census data (Figure 3, Supp. Figure
408 2). This is consistent with evidence from Vietnam and elsewhere^{62,63} and is likely mediated by
409 the ability and propensity to store water around homes when water supply is low or unreliable
410 (see below).

411 Notably, the negative effects of long-term urban expansion and built-up land suggest that – after
412 accounting for mobility and infrastructure – dengue incidence declines in increasingly urbanized
413 landscapes. This appears counterintuitive given that urban growth is typically considered a key
414 dengue driver (although systematic reviews have not shown clear empirical consensus for this
415 relationship^{6,25}). However, our satellite-based metrics are probably better indicators of formally-
416 planned urban developments than of more informal or peripheral settlement expansion, which
417 can be harder to detect from space⁶⁴. Such developments may generally have better provision of
418 water, sanitation and vector control services; as such, these results are consistent with our
419 infrastructure findings in suggesting that socio-environmental characteristics are the key
420 determinants of heterogeneity in risk across large areas. Taken together, these results suggest
421 that dengue incidence in Vietnam probably peaks in semi-urbanized or peri-urban areas – i.e.
422 relatively well-connected localities with extensive landscape modification for essential

423 sanitation, water and drainage, but lacking higher-quality infrastructure and services that could
424 otherwise reduce vector densities. Interestingly, this conclusion is supported by an earlier cohort
425 and modelling study from Vietnam that suggested susceptibility to large dengue outbreaks is
426 highest in areas with intermediate population densities and low piped water access⁶².

427 **Interacting effects of climatic and socio-environmental drivers on dengue dynamics**

428 We found strong evidence that temperature drives the spatial limits and temporal dynamics of
429 dengue across Vietnam. The nonlinear effect of monthly T_{mean} , peaking around 27°C, is
430 consistent with evidence from vector biology²⁶ and modelling studies³⁷. Notably, temperature of
431 the coolest month of the year explained the gradient in transmission intensity across Vietnam
432 (Supp. Figure 7), strongly suggesting that constraints on viral and mosquito persistence in cooler
433 months are barriers to endemic establishment in the north. Indeed, phylogeographic studies
434 have shown that transmission chains rarely persist over winter, and that yearly case surges in
435 northern Vietnam (including Ha Noi) are mainly seeded by reintroductions from the south⁴².
436 Consistent with this, we found markedly larger effect sizes and predictive influence of human
437 mobility in the north, which may reflect the importance of higher connectivity in facilitating
438 annual DENV reintroductions (Figure 5a). Smaller effects of mobility in the south might reflect
439 that populations are sufficiently large, and the climate consistently suitable, to support sustained
440 local transmission. More generally, these results suggest that highly-connected localities in
441 climatically-marginal regions may be useful targets for early surveillance, as dengue expansion is
442 likely to proceed via establishment in these areas before radiating outward^{65,66}. Our analyses
443 were constrained by imprecise mobility metrics (Table 1), and more detailed data sources (such
444 as transport networks or mobile phone data) could provide further insights into these expansion
445 dynamics¹⁴.

446 There is a need to understand how climatic variability and extreme weather events interact with
447 local socioeconomic contexts to drive outbreak dynamics, rather than considering climate
448 hazards as independent drivers^{38,67}. Our finding that hydrometeorological dynamics are
449 significant, multi-scalar drivers of dengue risk in Vietnam (Figure 3) adds to an emerging
450 evidence consensus for general effects of drought on dengue, as similar long-lag drought effects
451 have also been observed in Latin America and the Caribbean^{36,37}. Expanding on those studies, we
452 found that high improved water supply coverage changes the functional shape of the dengue-
453 SPEI-6 relationship, buffering against risk during low amplitude dry periods and sharply
454 increasing risk during severe drought (Figure 6). This is strongly indicative of a mediating role of
455 water storage practices. During slightly dry periods, piped or borehole-derived water supply may
456 decrease the need to store water in containers, and/or increase the frequency of stored water
457 replacement, both of which reduce vector production rate⁶⁸. In contrast, improved supply during
458 drought may increase the availability and propensity to store water in containers, whereas
459 households with lower access might switch to alternative sources such as bought water (as
460 suggested by past research in the Mekong Delta⁵⁹). Our water infrastructure metric did not
461 include service reliability or sociocultural perceptions of water quality and reliability, all of which
462 impact water usage and storage norms^{59,69}, and the inference of extreme drought effects by
463 nature relied upon a relatively small number of observations (Figure 6c). Nonetheless, including
464 this interaction improved spatial and temporal predictive accuracy, particularly in the highest-
465 burden southern provinces (Supp. Figure 18). This has implications for spatial prioritization of

466 interventions (e.g. vector control) to localities where water storage is highest during dry or
467 drought periods, as well as highlighting that developing accurate local-scale dengue forecasts
468 will likely need to account for complex climate-socioeconomic interactions.

469 **The role of environmental change in driving long-term dengue emergence in Vietnam**

470 Reported dengue burden has grown in many regions of Vietnam over the last two decades,
471 including northward expansion into central regions and the Red River Delta¹¹ (Figure 1b). Our
472 findings strongly suggest that recent socio-environmental and climatic changes have contributed
473 to this emergence trend, although we caution that our approach does not attribute observed
474 trends to changes in specific drivers. Notably, while most studies of dengue and climate change
475 have focused on future scenario-based projection^{34,70}, we instead used historical reanalysis data
476 which suggests that climate change in recent decades has already expanded and redistributed
477 transmission risk, likely facilitating dengue's northward spread (Figure 5, Supp. Figure 15). In the
478 north, the combined effects of a lengthening transmission season and rapid rises in mobility (up
479 to 14-fold since 1998) have probably contributed substantially to the emergence of dengue as an
480 annual problem in Ha Noi and the Red River Delta. Evidence of reductions in risk during the
481 hottest months, however, suggest that future climate change will have complex effects on
482 spatiotemporal patterns of dengue burden. Our approach stops short of attributing these effects
483 to anthropogenic climate forcing, instead comparing present-day risk patterns to a reference
484 period preceding the recent global temperature uptick; applying a formal detection and
485 attribution framework will be an important next step towards quantifying the anthropogenic
486 fingerprint on dengue burden⁷¹.

487 Recent changes in infrastructure have probably had complex effects on the landscape of dengue,
488 with transmission risk simultaneously increased via widespread expansion of sanitation systems
489 and reduced via growth of cities and improvements in water supply. Indeed, rather than a simple
490 positive dengue-urbanization relationship, localities most vulnerable to outbreaks are probably
491 peri-urban and transitional landscapes with increasingly dense populations but relatively weak
492 infrastructure and services. Our findings consequently support improvements in hygienic water
493 supply infrastructure as a pillar of climate adaptation to increasing mosquito-borne arboviral
494 risks, but also highlight potential limits to this adaptation. Climatic changes are stressing water
495 security in much of Southeast Asia, including Vietnam which has recently experienced severe
496 droughts and saltwater incursion, and regional drought risks are projected to increase in
497 future^{72,73}. Expanding access to improved water supply infrastructure may mitigate dengue risks
498 during dry periods, but might be insufficient to reduce dengue risks during severe droughts
499 without additional improvements to household water security. More broadly, our study shows the
500 value of integrating explanatory (hypothesis-driven) and predictive methods to understand the
501 interacting effects of climate and socioeconomic factors on emerging diseases.

502

503

504

505

506 **Materials & Methods**

507 **Dengue surveillance data**

508 Since 1998 Vietnam has maintained a dedicated national dengue passive surveillance system.
509 Data on monthly dengue case counts from May 1998 to April 2021 at administrative level 2
510 (“*districts*”) were collected and collated at the Pasteur Institute Ho Chi Minh City (Southeast and
511 Mekong River Delta provinces), Pasteur Institute Nha Trang (Central coastal provinces), Tay
512 Nguyen Institute of Hygiene and Epidemiology (Central Highlands provinces) and National
513 Institute of Hygiene and Epidemiology in Ha Noi (Northern provinces), with time-series beginning
514 between 1998 and 2002 depending on the region (Supp. Figure 1). Case counts were based on
515 passive surveillance using the national dengue case definition, and include both laboratory-
516 confirmed and suspected cases. Other infections, particularly arboviruses, could be
517 misdiagnosed as suspected dengue cases; however, reported case numbers and seroprevalence
518 estimates for chikungunya and Zika in Vietnam have been relatively low^{74,75}, so this would be
519 unlikely to substantially impact inference. Currently there are 713 districts in Vietnam, although a
520 substantial number of these were established through redrawing of administrative boundaries
521 since 1998; to ensure geographical comparability throughout the study period, we combined
522 dengue case counts for 46 districts to match their 1998 boundaries, creating a final dataset of
523 174,936 monthly case counts from 667 districts (Figure 1a, Supp. Figure 1). Case counts were
524 assigned to a dengue transmission year (from April to May) for modelling.

525 **Socio-environmental and climatic covariates**

526 We developed spatially- and temporally-explicit covariates to represent hypothesized drivers of
527 dengue transmission and spread (Table 1). Covariates are visualised in Supp. Figures 2-3, and
528 data sources and processing are summarized below (for full description see Supp. Table 1 and
529 Supp. Text 1). Raster data extraction and processing was conducted using ‘sf’, ‘raster’ and
530 ‘exactextract’ in R 4.0.3⁷⁶⁻⁷⁸. We accessed population data (total and density) from census-
531 based data, urbanization metrics (built-up land extent, and expansion rate in preceding 3- and 10-
532 year windows) from satellite data⁴⁸, and infrastructure metrics (% households with access to
533 hygienic toilet, and % piped or borehole-derived water) from the Vietnam Population and Housing
534 Census (2009 and 2019, interpolated and projected to annual values). We accessed province-
535 level annual road travel rates (km per inhabitant reported by the Vietnam General Statistics
536 Office) as a measure of observed levels of population movement. In the absence of detailed
537 mobility data such as mobile phone records, we used parameter-free gravity and radiation
538 models to predict annual district-level relative connectivity (predicted mean population flux),
539 based on population data and pairwise travel times between all pairs of districts^{15,79}.

540 Monthly temperature indicators (monthly mean T_{mean} , T_{min} and T_{max}) were derived from ERA5-
541 Land reanalysis data^{49,80,81}. Since broad climatic suitability gradients could confound
542 relationships with other variables, we also calculated three annual temperature indicators to
543 represent more fundamental constraints on dengue persistence (annual mean T_{mean} , annual
544 mean T_{min} , T_{mean} of the coolest month). Monthly precipitation indicators were derived from bias-
545 adjusted ERA5 data (WFDE5; Supp. Figure 3-4). In addition to precipitation, we used the R
546 package ‘spei’⁵¹ to estimate multi-scalar drought indicators (Standardised Precipitation
547 Evapotranspiration Index; SPEI) from 40 year timeseries of monthly WFDE5 precipitation and

548 ERA5-Land potential evapotranspiration in each district (reference period 1981-2020). SPEI
549 incorporates effects of both precipitation and evapotranspiration on water availability^{52,53}, with
550 values above and below 0 indicating, respectively, surface water excess or deficit relative to the
551 long-term historical average in a given seasonal time window (for example, a 6-month SPEI for
552 Jan-Jun 2018 would compare to Jan-Jun in all other years). SPEI values denote the relative
553 magnitude of this deviation, from near-normal to moderate (absolute values from 0 to 1), from
554 moderate to severe (absolute values 1 to 2), to extreme wet/dry conditions (absolute values >2).
555 We estimated monthly SPEI within 1-month, 6-month and 12-month windows to capture varying
556 timescales of drought (SPEI-1 as short-timescale; SPEI-6 and SPEI-12 as long-timescale).
557 Climatic covariates were derived at lags of 0 to 6 months prior to the focal month to account for
558 delayed effects (Supp. Text 1).

559 **Statistical model development**

560 To infer relationships between covariates and dengue incidence we fitted spatiotemporal models
561 in a Bayesian framework (integrated nested Laplace approximation, in INLA 21.7.10.1^{82,83}).
562 Monthly dengue case counts $Y_{i,t}$ ($n=174,936$) were modelled as a negative binomial process to
563 account for overdispersion:

$$564 \quad Y_{i,t} \sim \text{NegBinom}(\mu_{i,t}, n)$$

565 where n is the size (overdispersion) parameter and $\mu_{i,t}$ is the expected mean number of cases
566 for district i during month t , modelled as a log link function of the following general linear
567 predictor:

$$568 \quad \log(\mu_{i,t}) = \alpha + P_{i,t} + \rho_{r(i),t} + u_{i,y(t)} + v_{i,y(t)}$$

569 Here, α is the intercept and $P_{i,t}$ is log population included as an offset. $\rho_{r(i),t}$ is a province-
570 specific effect of calendar month to account for geographic variability in dengue seasonality
571 (districts i are nested within 63 provinces r), specified as a cyclic first-order random walk to
572 capture dependency between successive months. To account for unexplained variation in
573 spatiotemporal patterns of dengue across Vietnam (due to unmeasured factors such as
574 population immunity), $u_{i,y(t)}$ and $v_{i,y(t)}$ are dengue year-specific (23 years, y) spatially-structured
575 (conditional autoregressive; u) and unstructured (i.i.d; v) district-level random effects, jointly
576 specified as a Besag-York-Mollie model⁵⁵.

577 We fitted the above random effects-only model as a baseline (Supp. Figure 5), and conducted
578 model selection to develop a multivariate model including population, climate, urbanisation,
579 infrastructure and mobility covariates (Table 1). We compared models using within-sample
580 information criteria: Watanabe-Akaike Information Criterion (WAIC), Deviance Information
581 Criterion (DIC) and cross-validated logarithmic score (log-score; calculated from the pointwise
582 conditional predictive ordinate, an approximation of leave-one-out cross-validation). Comparing
583 variation explained between different models using metrics such as pseudo- R^2 was not
584 particularly informative, as the district-level random effects ($u_{i,y(t)} + v_{i,y(t)}$) are at the same
585 annual resolution as most covariates (Table 1), and thus tend to compensate for excluded
586 variables. We instead calculated measures of unexplained random effects variation (mean
587 absolute error in district-level or seasonal effects), which indicates how much these effects
588 attenuate towards zero when covariates are included. We first selected each covariate's best-

589 fitting type (either T_{mean} , T_{min} or T_{max} for monthly temperature; either SPEI-6 or SPEI-12 for long-
590 timescale drought; gravity or radiation; 3- or 10-year urban expansion), functional form (linear,
591 logarithmic or nonlinear, the latter specified as a second-order random walk) and lag (climate
592 variables only) by adding each individually to the baseline model and comparing WAIC (Supp.
593 Figure 6). Covariates considered for inclusion in a full multivariate model were: fixed effects of
594 T_{mean} coolest month, log population density, log gravity flux, log road traffic per inhabitant, built-
595 up land, log 10-year urban expansion rate, and nonlinear effects of hygienic toilet access, piped
596 water access, T_{mean} 1-month lag, SPEI-1 1-month lag and SPEI-6 5-month lag.

597 Owing to the dataset's large size and the expectation of confounding relationships among
598 covariates, it was both undesirable and computationally unfeasible to conduct a programmatic
599 covariate selection process. Instead we conducted a more limited model comparison procedure
600 to develop a final multivariate model. To do this, we first excluded covariates with evidence of
601 substantial multicollinearity when tested using variance inflation factors (log population density
602 and log gravity flux were highly collinear, and the former was excluded because gravity flux
603 improved models more during individual covariate analysis; Supp Figure 6). We then fitted a
604 multivariate model including all 10 remaining covariates and compared this to 10 separate
605 models each holding out 1 covariate at a time. Covariates whose inclusion did not improve
606 model fit according to at least 2 of the 3 within-sample metrics (WAIC, DIC and log-score) were
607 excluded. All covariates improved the model by this majority rule criterion, and were retained.

608 We examined residuals and conducted posterior predictive checks to check the model met
609 distributional assumptions. We also conducted a sensitivity analysis based on degree of
610 urbanisation because, despite relatively low collinearity overall (Supp. Figure 2), many large cities
611 cluster with relatively high values for many key covariates. Since this could affect parameter
612 estimates, we tested sensitivity by sequentially re-fitting the model holding out all observations in
613 areas with >90%, >70% or >50% of population residing in urban areas as defined from census
614 data (i.e. fitting the model to data from increasingly rural settings). To examine whether socio-
615 environmental effects differ substantially between endemic and emerging dengue transmission
616 settings, we also separately fitted the final multivariate model to data from southern Vietnam
617 (Mekong River Delta, Southeast, South Central Coast and Central Highlands) and northern
618 Vietnam (North Central, Red River Delta, Northeast and Northwest).

619 **Measuring covariate predictive influence through block cross-validation tests**

620 Inference can be strengthened through combining explanatory and predictive approaches, for
621 example by using structured predictive tests to challenge the ability of hypothesis-led
622 explanatory models to predict unseen observations^{56,57} (i.e. testing the generalisability of inferred
623 relationships). For strongly spatially-dependent phenomena such as disease incidence, block
624 cross-validation designs –which hold out data in spatially- or temporally-structured blocks – are
625 more appropriate than fully randomised approaches⁸⁴, and can provide insights into how
626 different variables contribute to predicting different dimensions of a phenomenon (Supp. Figure
627 8). To estimate the influence of individual covariates on predicting spatial and temporal
628 variability in dengue incidence, we conducted block cross-validation experiments to estimate
629 out-of-sample (OOS) prediction error for the baseline model, full model, and 10 models each
630 excluding a single covariate from the full model. In each run, the dataset was 5-fold partitioned

631 (observations were randomly allocated to folds following a given block holdout design, as
632 described below) and OOS predictions were generated for each model using 80%-20% train-test
633 splits (i.e. across 5 submodels). Prediction error (difference between observed and predicted
634 cases) was summarised as mean absolute error (MAE_{OOS}), across all observations, at district-
635 level and, to examine differences between regions, across all observations within either southern
636 or northern Vietnam (Supp. Figure 11-12)

637 This procedure was repeated 10 times each for 3 block holdout designs⁸⁴ to account for
638 variation associated with random allocation of folds (Supp. Figure 8a-b). *Spatial*: 5-fold of
639 complete districts, i.e. predicting full dengue incidence time series in completely unobserved
640 areas. *Spatiotemporal*: 5-fold of district-year combinations, i.e. predicting completely unobserved
641 years in partially observed locations. *Seasonal*: 5-fold of quarterly (3-month) blocks per-district,
642 i.e. predicting unobserved intra-annual epidemic dynamics. Under spatial and spatiotemporal
643 holdout designs, the expected magnitude of dengue incidence in unobserved locations and years
644 is inferred from nearby observed locations, via the spatially-structured effects $u_{i,y(t)}$ (Supp.
645 Figure 8c). These designs therefore test the contribution of covariates to predicting spatial
646 heterogeneity in dengue incidence dynamics among nearby locations (i.e. differences from the
647 expected similarity to neighbouring districts). Under the seasonal block design, the random
648 effects contain information about the expected magnitude of cases in unobserved blocks,
649 inferred from other observations in the same district and year (Supp. Figure 8d). This design
650 therefore tests the contribution of monthly climatic variability to predicting departures from this
651 seasonal expectation (Supp. Figure 8d).

652 **Examining the recent impacts of climate change using historical temperature data**

653 To examine the possible contribution of recent climate change to dengue expansion patterns
654 nationally, we used the inferred risk function of monthly temperature (T_{mean} 1-month lag; Figure
655 3e) to project monthly posterior mean temperature-driven dengue risk since 1950 for all districts,
656 using long-term T_{mean} data from ERA5-Land reanalysis. To do this, we used the fitted risk
657 function to predict the monthly marginal effect of T_{mean} on dengue incidence (i.e. while holding
658 all other variables constant) for each month across the full historical time-series. To visualise
659 present-day risk dynamics in space and time, we then summarised and mapped 20-year means
660 of monthly district-level risk for the period 2001-2020. To test for effects of climate change, we
661 compared 20-year average risk between a historical reference period (1951-1970) and the
662 present-day period, per-district and month, using linear models with time period as a categorical
663 covariate. The use of 20-year averages was to account for natural climate system variability. The
664 historical reference period was based on the earliest available ERA5-Land data, and while not
665 reflective of the pre-industrial baseline, precedes the sharp acceleration of global temperatures
666 that has occurred since around 1970. Climate reanalysis is based on assimilating observational
667 data with climate models to provide a detailed and accurate reconstruction of historical climate
668 dynamics, and its accuracy relies upon observational data. The number of observations
669 assimilated by ERA5 increases tenfold between 1950 and 1970, and this lower data coverage
670 might reduce accuracy in earlier years⁵⁸; we therefore also tested the sensitivity of results to
671 defining a later reference period (1971-1990) when coverage is much higher.

672 **Examining multi-scalar effects of drought, and interactions with infrastructure, in southern** 673 **Vietnam**

674 We extended the full model to investigate the effects of interactions between extreme
675 wetness/drought and local infrastructure on dengue incidence, over multiple timescales and
676 delays (from 0 to 6 months), focusing on endemic southern Vietnam. We examined the
677 relationship between SPEI and dengue incidence, and improvements in model fit, for all lags and
678 timescales of SPEI (SPEI-1 and SPEI-6 at 0 to 6 months delay), by including each metric
679 individually in the full model containing all covariates except SPEI. To test the hypothesis that the
680 effects of drought on dengue are mediated by water supply, we tested whether models were
681 improved by stratifying the best-fitting short-timescale (SPEI-1 1-month) and long-timescale
682 (SPEI-6 5-month) drought indicator by either level of improved water access or urbanization
683 (grouped as low, intermediate, or high, defined as <25%, 25-75% or >75% respectively). We
684 expected that stratification of the SPEI-6 effect by water supply would improve models more
685 than stratifying SPEI-1, and that stratifying by water supply would improve models more than
686 stratifying by urbanization (Results). We used information criteria as described above (WAIC, DIC
687 and log-score) to evaluate whether including each interaction improved model fit compared to
688 the full (non-interaction) model. For each model we also tested whether interactions reduced
689 OOS prediction error under spatiotemporal and seasonal cross-validation, as described above.

690 **Data and code availability**

691 The data and code pipeline used for this study are available at:
692 https://github.com/rorygibb/dengue_vietnam_ms. To demonstrate pipeline functionality the
693 repository contains dengue data for a subset of Vietnamese provinces. The full dengue
694 incidence data underlying these results are available from: Phan Trong Lan, General Department
695 of Preventive Medicine, MOH, email: phantronglan@gmail.com

696 **Acknowledgements**

697 The authors thank Colin Carlson for insightful discussion of early results. This research was
698 supported by the UK Space Agency-funded International Partnership Programme 2 D-MOSS
699 project "*An integrated dengue early warning system driven by Earth Observations in Vietnam*" (all
700 authors), as well as a Royal Society Dorothy Hodgkin Fellowship (RL), a Wellcome Trust Sir Henry
701 Wellcome Fellowship (206471/Z/17/Z) and a UK Medical Research Council Career Development
702 Award (MR/V031112/1, both OB).

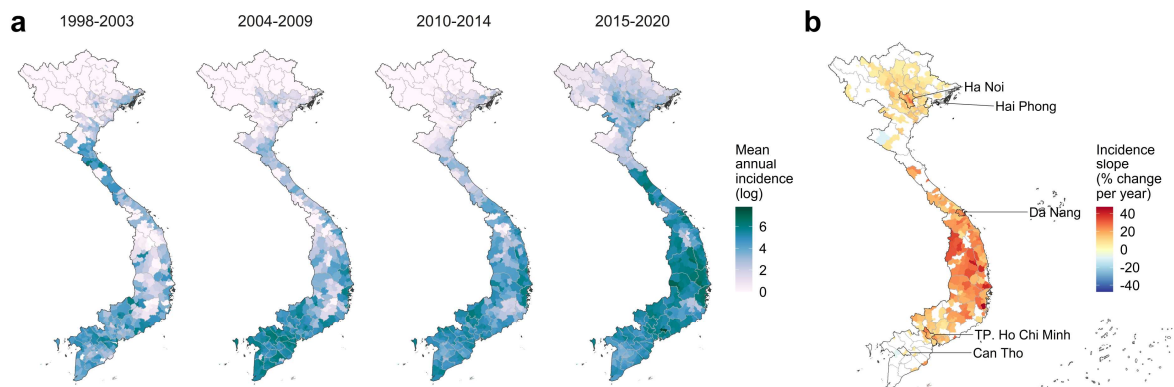
703 **Author contributions**

704 Initial concept: RG, OB, RL.
705 Analysis design: RG, FC-G, OB, RL
706 Data collection: PTL, PTH, VSN, VTD, DTH, NTD, VCC, LT, DKQ, TMH, NHT, TTH
707 Data collation and processing: RG, VTD, NTD, LT, DKQ, GT, BH
708 Data analysis and modelling: RG
709 Writing (initial draft): RG
710 Writing (review and editing): All authors
711 Funding: RL, OB, GT, DL
712 Project administration: GT, DL

713 **Competing interests:** We declare that no competing interests exist.

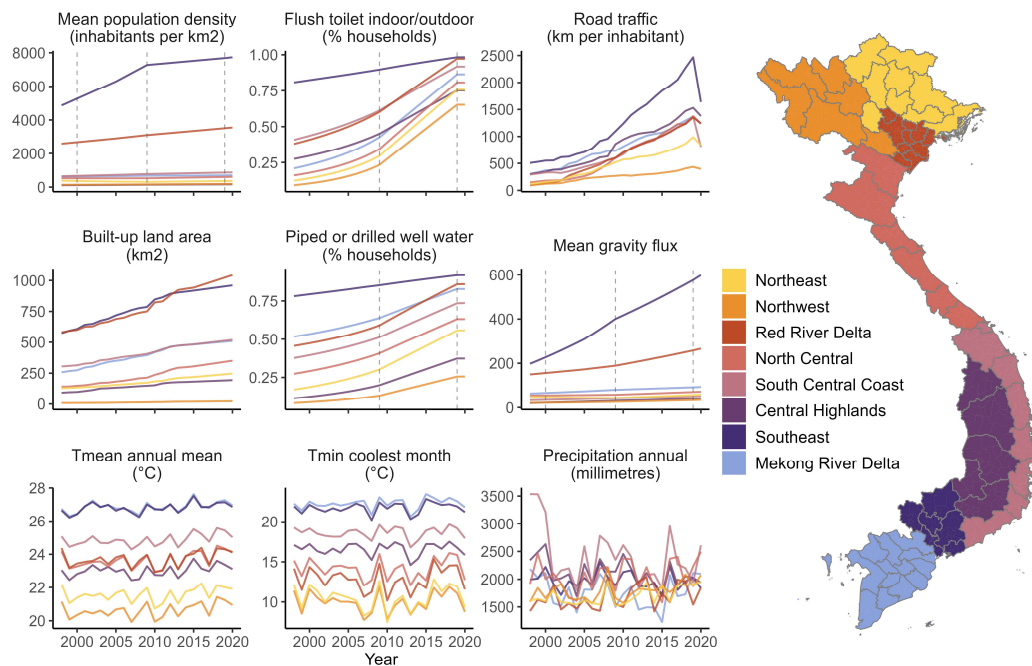
714 **Figures and Tables**

715 **Figure 1: Geographical distribution and trends in dengue incidence at district-level in Vietnam.**
716 (A) Mean annual dengue incidence rates across all dengue years (May to April) within each 5-6
717 year time period between 1998 – 2020 (cases per 100,000 persons, log+1 transformed for
718 visualization purposes) for districts with dengue time series available (n=667). (B) Estimated
719 slopes of annual dengue incidence rates between 1998 and 2020 (% change per year) for
720 districts with strong evidence ($p < 0.01$) of increasing (red) or decreasing (blue) trends, with
721 Vietnam's 5 major urban municipalities labelled. The latitudinal gradient in seasonal dynamics is
722 shown in Supp. Figure 1.

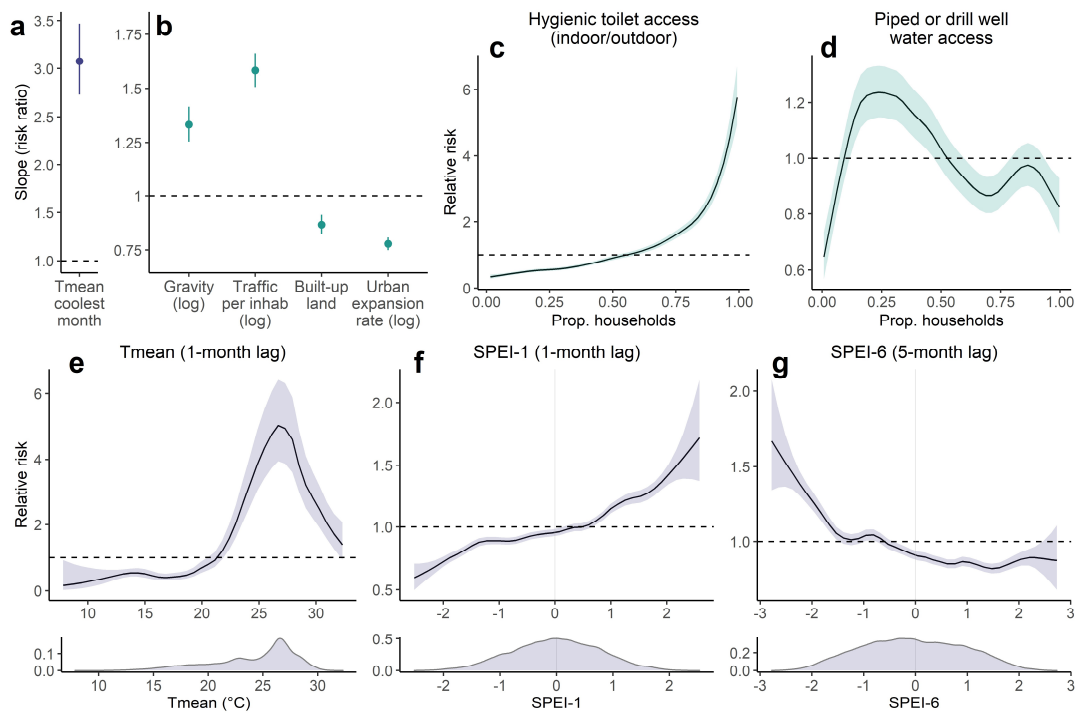


723
724
725
726
727
728
729
730
731
732
733
734
735
736
737
738
739
740
741

742 **Figure 2: Socio-environmental change and climatic variability in Vietnam from 1998 to 2020.**
743 Sub-plots show annual socio-environmental and climatic covariate data (Table 1), aggregated
744 from district- to region-level for visualization (region denoted by line and map fill colour;
745 population density, gravity flux, temperature and precipitation are summarized as the mean
746 across all districts). For census-based metrics (population, infrastructure, and gravity models)
747 annual estimates were obtained via district-level interpolation or back/forward projection from
748 observed years, which are shown as dotted lines (Methods, Supp. Text 1). For all other metrics,
749 data were available for all years. Urbanization, population density and mobility are highest in the
750 subregions with the two largest municipalities: Ha Noi (Red River Delta) and Ho Chi Minh City
751 (Southeast).



766 **Figure 3: Effects of socio-environmental and climatic drivers on district-level dengue incidence.**
 767 Sub-panels show posterior marginal linear fixed effects (A-B) and nonlinear effects (C-G) from
 768 the full fitted model of district-level dengue incidence (n=667 districts, 174,936 observations;
 769 Methods). Linear fixed effects are shown as risk ratios for scaled or log-transformed covariates
 770 (i.e. proportion change in risk for a 1 unit change in covariate), with points and error bars
 771 showing posterior marginal mean and 95% credible interval. Nonlinear marginal effects
 772 (specified as second-order random walks; Methods) are shown on the relative risk scale, with
 773 lines and ribbons showing posterior mean and 95% credible interval. Point or ribbon colour
 774 denotes broad covariate class: either socio-environmental (green) or climatic (blue).



775

776

777

778

779

780

781

782

783

784

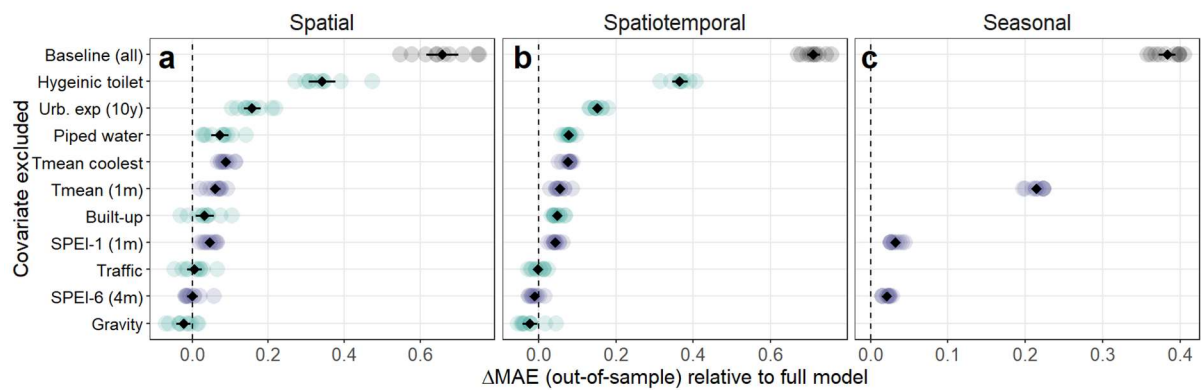
785

786

787

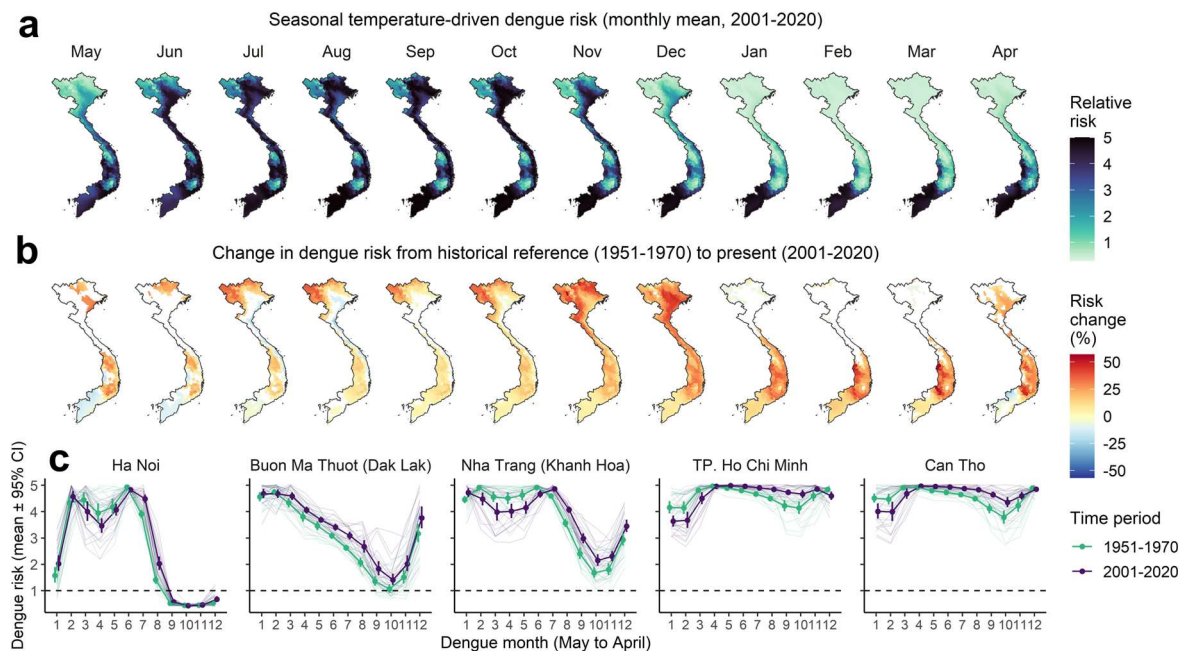
788

789 **Figure 4: Influence of individual socio-environmental and climatic factors on spatiotemporal**
 790 **and seasonal predictions of dengue incidence.** Influence of individual covariates on out-of-
 791 sample mean absolute error (MAE) was evaluated using 5-fold cross validation under 3 block
 792 holdout designs: spatial (entire districts), spatiotemporal (district-year combinations) and
 793 seasonal (quarterly blocks within each district) (Methods, Supp. Figure 8). Candidate models
 794 excluding one covariate at a time from the full model are shown on the y axis, with the baseline
 795 (random effects-only) model for comparison. Individual points show change in MAE relative to
 796 the full model (dashed line), across 10 repeats account for variability due to random reallocation
 797 of cross-validation folds. Point colour denotes broad covariate class: socio-environmental
 798 (green), climatic (blue) or baseline model (grey). Black points and error bars summarise the
 799 mean and 95% confidence interval across all 10 repeats. Values above zero indicate an increase
 800 in prediction error relative to the full model when a covariate is excluded (i.e. positive influence
 801 on prediction accuracy), and vice versa.



802
803
804
805
806
807
808
809
810
811
812
813
814
815
816
817
818

819 **Figure 5: Recent climate change has expanded and redistributed dengue transmission risk**
 820 **across Vietnam.** The full model was used to predict monthly marginal temperature-driven risk
 821 since 1950 using ERA5-Land reanalysis data (i.e. holding all other variables constant). Top maps
 822 (A) show present-day monthly 20-year means of dengue relative risk (2001-2020), with darker
 823 colours denoting increased risk. Bottom maps (B) show the monthly percentage difference in 20-
 824 year average dengue risk between historical reference (1951-1970) and present-day (red
 825 shading denotes increasing risk and blue decreasing risk). Only statistically significant
 826 differences ($p < 0.05$) are shown, with non-significant differences shaded white. Graphs (C) show
 827 long-term changes in seasonal risk by dengue month (May to April) for 5 example cities with high
 828 dengue burden (Ha Noi in north; Buon Ma Thuot in the central highlands; Nha Trang on the south
 829 central coast; and Ho Chi Minh and Can Tho in the south). Fine lines show individual years, and
 830 points and error-bars show monthly 20-year mean and standard error, with lines coloured by time
 831 period (green for reference period; purple for present-day). The supplementary material shows
 832 more district examples (Supp. Figure 13) as well as changes in temperature patterns for these 5
 833 localities (Supp. Figure 14). Results were very similar when defining a later reference period
 834 (1971-1990; Supp. Figure 15).



835

836

837

838

839

840

841

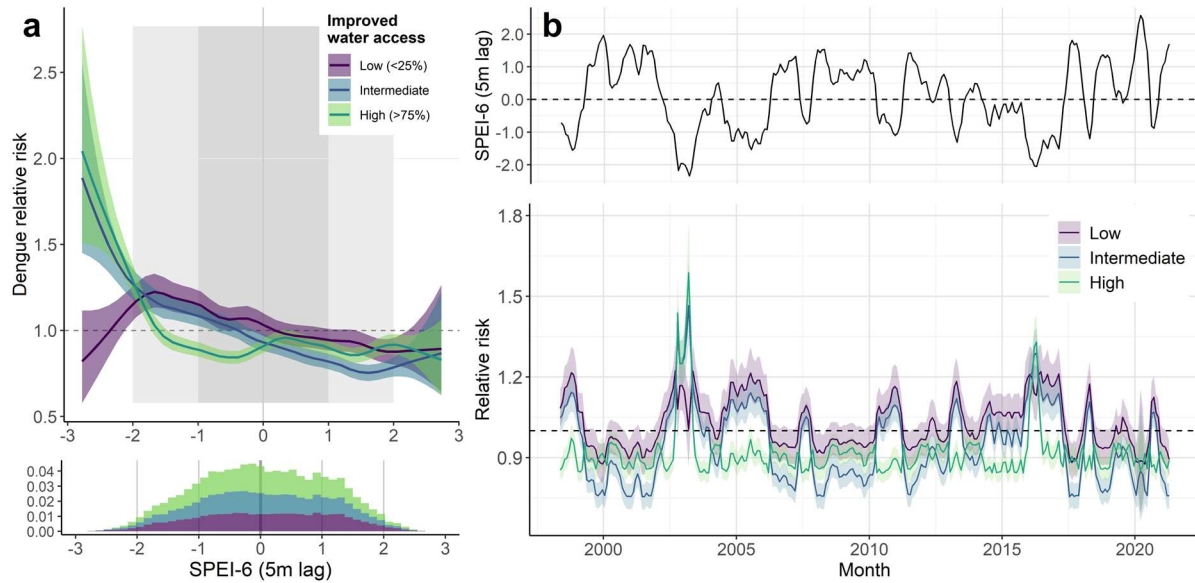
842

843

844

845

846 **Figure 6: Improved water supply modifies the effect of long-term drought (SPEI-6) on dengue**
847 **incidence in southern Vietnam.** The fitted interaction between SPEI-6 (5-month lag) and piped or
848 drilled well water access is shown in A (low= $<25\%$ of households; medium= $25\text{--}75\%$, high= $\geq 75\%$),
849 with lines and shaded area showing posterior marginal mean and 95% credible interval.
850 Histogram shows the distribution of observations across the 3 strata (bar height is cumulative
851 across 3 strata). Visualisation of the marginal effect of SPEI-6 on relative risk is shown in B, for
852 an example time series of SPEI-6 from the Mekong River Delta region (top row; Dong Thap
853 province), under scenarios of low, intermediate and high improved water access (bottom row).
854 Accounting for this interaction reduces predictive error under both spatiotemporal and seasonal
855 cross validation (Supp. Figure 16-17).



856
857
858
859
860
861
862
863
864
865
866
867
868
869
870

871 **Table 1: Climatic and socio-environmental covariates as hypothesized drivers of dengue**
 872 **incidence.** The table lists covariates used in models, their broad class, data sources, and
 873 rationale for testing. A fuller description of covariate sources, original data resolution and
 874 processing are provided in Supp. Table 1, Methods and Supp. Text 1. Acronym definitions: ERA5-
 875 Land (ECMWF Reanalysis v5 over land), WFDE5 (bias-adjusted ERA5 reanalysis precipitation
 876 data with reference to GPCP and CPC station data), VGSO (Vietnam General Statistics Office).

Covariate	Type	Source	Rationale
Annual temperature (mean and coolest month)	Climate (temperature)	ERA5-Land ⁴⁹	Geographical limits on dengue virus persistence and transmission by mosquitoes ³⁴ . Warmer annual temperatures are expected to facilitate year-round transmission.
Monthly temperature	Climate (temperature)	ERA5-Land ⁴⁹	Impacts spatial and seasonal biophysical suitability for DENV transmission ²⁶ . Relationship may be nonlinear and depend on time delay.
Precipitation	Climate (hydrometeorology)	WFDE5 v2.1. ⁵⁰	Impacts seasonal creation and flushing of <i>Aedes</i> breeding sites. Relationship may be nonlinear and depend on time delay.
Standardised Precipitation Evapotranspiration Index (SPEI) in 1-month, 6-month and 12-month windows	Climate (hydrometeorology)	Derived from WFDE5 using 'spei' package ⁵²	Measures deviations from historical average hydrometeorological conditions for reference period 1981-2020 (i.e. excess or deficit), from short- to long timescales, so may be more sensitive to local context than simple precipitation. Relationship may be nonlinear and depend on time delay ³⁶ .
Built-up land	Urbanisation	ESA-CCI land cover (annual)	More built-up land is expected to increase availability of highly suitable <i>Aedes</i> habitat.
Urban expansion rate (3-year and 10-year window)	Urbanisation	Landsat urban dynamics ⁴⁸ (annual)	Short-term (i.e. construction phase) and rapid or informal longer-term expansion of built environment may increase availability of suitable <i>Aedes</i> habitat.
Hygienic toilet access (indoor/outdoor flush toilet)	Infrastructure	Vietnam census 2009 and 2019 (interpolated to annual values)	Improved sanitation systems may reduce density of standing water for vector breeding sites, and therefore reduce transmission.
Improved water access (piped or drilled well water)	Infrastructure	Vietnam census 2009 and 2019 (interpolated to annual values)	Higher access may reduce propensity to store water around homes, reducing vector breeding sites and thus transmission.
Population density	Population	Gridded Population of the World 2000 and Vietnam census 2009 and 2019 (interpolated to annual values)	Higher population density is expected to lead to increasing contact rates and potential for long-term persistence of transmission chains, so may increase incidence.
Road traffic per inhabitant	Mobility	VGSO (annual, province-level)	Higher rates of within-province population movements are expected to increase local dengue spread.
Potential population fluxes (mean gravity and radiation flux)	Mobility	Gravity and radiation models (applied to annual population)	Model-based proxy for relative attractiveness of districts for population movement (e.g. commuting). Higher movement rates are expected to increase rates of influence dengue introduction and spread.

877

878

879

880 References

- 881 1. Romanello, M. *et al.* The 2021 report of the Lancet Countdown on health and climate change: code red for a
882 healthy future. *The Lancet* **398**, 1619–1662 (2021).
- 883 2. Mora, C. *et al.* Over half of known human pathogenic diseases can be aggravated by climate change. *Nat.*
884 *Clim. Chang.* **12**, 869–875 (2022).
- 885 3. Baker, R. E. *et al.* Infectious disease in an era of global change. *Nat Rev Microbiol* **20**, 193–205 (2022).
- 886 4. Wilder-Smith, A. *et al.* Epidemic arboviral diseases: priorities for research and public health. *The Lancet*
887 *Infectious Diseases* **17**, e101–e106 (2017).
- 888 5. Brady, O. J. & Hay, S. I. The Global Expansion of Dengue: How *Aedes aegypti* Mosquitoes Enabled the First
889 Pandemic Arbovirus. *Annu. Rev. Entomol.* **65**, 191–208 (2020).
- 890 6. Kolimenakis, A. *et al.* The role of urbanisation in the spread of *Aedes* mosquitoes and the diseases they
891 transmit—A systematic review. *PLoS Neglected Tropical Diseases* **15**, e0009631 (2021).
- 892 7. Stanaway, J. D. *et al.* The Global Burden of Dengue: an analysis from the Global Burden of Disease Study
893 2013. *Lancet Infect Dis* **16**, 712–723 (2016).
- 894 8. Jentes, E. S. *et al.* Evidence-based risk assessment and communication: a new global dengue-risk map for
895 travellers and clinicians#. *Journal of Travel Medicine* **23**, taw062 (2016).
- 896 9. Chareonsook, O., Foy, H. M., Teeraratkul, A. & Silarug, N. Changing epidemiology of dengue hemorrhagic fever
897 in Thailand. *Epidemiol Infect* **122**, 161–166 (1999).
- 898 10. Lowe, R. *et al.* Emerging arboviruses in the urbanized Amazon rainforest. *BMJ* m4385 (2020)
899 doi:10.1136/bmj.m4385.
- 900 11. Cuong, H. Q. *et al.* Quantifying the Emergence of Dengue in Hanoi, Vietnam: 1998–2009. *PLoS Negl Trop Dis* **5**,
901 e1322 (2011).
- 902 12. Cochet, A. *et al.* Autochthonous dengue in mainland France, 2022: geographical extension and incidence
903 increase. *Eurosurveillance* **27**, 2200818 (2022).
- 904 13. Rijal, K. R. *et al.* Epidemiology of dengue virus infections in Nepal, 2006–2019. *Infectious Diseases of Poverty*
905 **10**, 52 (2021).
- 906 14. Lee, S. A., Economou, T., de Castro Catão, R., Barcellos, C. & Lowe, R. The impact of climate suitability,
907 urbanisation, and connectivity on the expansion of dengue in 21st century Brazil. *PLoS Negl Trop Dis* **15**,
908 e0009773 (2021).
- 909 15. Wesolowski, A. *et al.* Impact of human mobility on the emergence of dengue epidemics in Pakistan. *PNAS*
910 **112**, 11887–11892 (2015).

- 911 16. Ryan, S. J., Carlson, C. J., Mordecai, E. A. & Johnson, L. R. Global expansion and redistribution of Aedes-borne
912 virus transmission risk with climate change. *PLOS Neglected Tropical Diseases* **13**, e0007213 (2019).
- 913 17. Gubler, D. J. Dengue, Urbanization and Globalization: The Unholy Trinity of the 21st Century. *Trop. Med. Health*
914 **39**, S3–S11 (2011).
- 915 18. Salje, H. *et al.* Dengue diversity across spatial and temporal scales: Local structure and the effect of host
916 population size. *Science* **355**, 1302–1306 (2017).
- 917 19. Salje, H. *et al.* Revealing the microscale spatial signature of dengue transmission and immunity in an urban
918 population. *PNAS* **109**, 9535–9538 (2012).
- 919 20. Raghwani, J. *et al.* Endemic Dengue Associated with the Co-Circulation of Multiple Viral Lineages and
920 Localized Density-Dependent Transmission. *PLOS Pathogens* **7**, e1002064 (2011).
- 921 21. Kache, P. A. *et al.* Bridging landscape ecology and urban science to respond to the rising threat of mosquito-
922 borne diseases. *Nat Ecol Evol* 1–16 (2022) doi:10.1038/s41559-022-01876-y.
- 923 22. Stoddard, S. T. *et al.* House-to-house human movement drives dengue virus transmission. *Proc Natl Acad Sci*
924 *U S A* **110**, 994–999 (2013).
- 925 23. Reiner, R. C., Stoddard, S. T. & Scott, T. W. Socially structured human movement shapes dengue transmission
926 despite the diffusive effect of mosquito dispersal. *Epidemics* **6**, 30–36 (2014).
- 927 24. Seidahmed, O. M. E., Lu, D., Chong, C. S., Ng, L. C. & Eltahir, E. A. B. Patterns of Urban Housing Shape Dengue
928 Distribution in Singapore at Neighborhood and Country Scales. *GeoHealth* **2**, 54–67 (2018).
- 929 25. Gao, P. *et al.* Land use and land cover change and its impacts on dengue dynamics in China: A systematic
930 review. *PLOS Neglected Tropical Diseases* **15**, e0009879 (2021).
- 931 26. Mordecai, E. A. *et al.* Thermal biology of mosquito-borne disease. *Ecology Letters* **22**, 1690–1708 (2019).
- 932 27. Power, G. M. *et al.* Socioeconomic risk markers of arthropod-borne virus (arbovirus) infections: a systematic
933 literature review and meta-analysis. *BMJ Global Health* **7**, e007735 (2022).
- 934 28. Telle, O. *et al.* Social and environmental risk factors for dengue in Delhi city: A retrospective study. *PLOS*
935 *Neglected Tropical Diseases* **15**, e0009024 (2021).
- 936 29. Nguyen-Tien, T. *et al.* Risk factors of dengue fever in an urban area in Vietnam: a case-control study. *BMC*
937 *Public Health* **21**, 664 (2021).
- 938 30. Barrera, R. *et al.* Unusual productivity of *Aedes aegypti* in septic tanks and its implications for dengue control.
939 *Medical and Veterinary Entomology* **22**, 62–69 (2008).
- 940 31. van Panhuis, W. G. *et al.* Region-wide synchrony and traveling waves of dengue across eight countries in
941 Southeast Asia. *PNAS* **112**, 13069–13074 (2015).

- 942 32. Rabaa, M. A. *et al.* Frequent In-Migration and Highly Focal Transmission of Dengue Viruses among Children in
943 Kamphaeng Phet, Thailand. *PLOS Neglected Tropical Diseases* **7**, e1990 (2013).
- 944 33. Colón-González, F. J. *et al.* Projecting the risk of mosquito-borne diseases in a warmer and more populated
945 world: a multi-model, multi-scenario intercomparison modelling study. *The Lancet Planetary Health* **5**, e404–
946 e414 (2021).
- 947 34. Messina, J. P. *et al.* The current and future global distribution and population at risk of dengue. *Nat Microbiol*
948 **4**, 1508–1515 (2019).
- 949 35. Caldwell, J. M. *et al.* Climate predicts geographic and temporal variation in mosquito-borne disease dynamics
950 on two continents. *Nat Commun* **12**, 1233 (2021).
- 951 36. Lowe, R. *et al.* Nonlinear and delayed impacts of climate on dengue risk in Barbados: A modelling study. *PLOS*
952 *Medicine* **15**, e1002613 (2018).
- 953 37. Lowe, R. *et al.* Combined effects of hydrometeorological hazards and urbanisation on dengue risk in Brazil: a
954 spatiotemporal modelling study. *The Lancet Planetary Health* **5**, e209–e219 (2021).
- 955 38. Santos-Vega, M., Martinez, P. P. & Pascual, M. Climate forcing and infectious disease transmission in urban
956 landscapes: integrating demographic and socioeconomic heterogeneity. *Ann N Y Acad Sci* **1382**, 44–55
957 (2016).
- 958 39. Wartel, T. A. *et al.* Three Decades of Dengue Surveillance in Five Highly Endemic South East Asian Countries:
959 A Descriptive Review. *Asia Pac J Public Health* **29**, 7–16 (2017).
- 960 40. Quyen, D. L. *et al.* Epidemiological, Serological, and Virological Features of Dengue in Nha Trang City, Vietnam.
961 *The American Journal of Tropical Medicine and Hygiene* **98**, 402–409 (2018).
- 962 41. Thai, K. T. D. *et al.* Seroprevalence of dengue antibodies, annual incidence and risk factors among children in
963 southern Vietnam. *Tropical Medicine & International Health* **10**, 379–386 (2005).
- 964 42. Rabaa, M. A. *et al.* Dengue Virus in Sub-tropical Northern and Central Viet Nam: Population Immunity and
965 Climate Shape Patterns of Viral Invasion and Maintenance. *PLOS Neglected Tropical Diseases* **7**, e2581
966 (2013).
- 967 43. Tsunoda, T., Chaves, L. F., Nguyen, G. T. T., Nguyen, Y. T. & Takagi, M. Winter Activity and Diapause of *Aedes*
968 *albopictus* (Diptera: Culicidae) in Hanoi, Northern Vietnam. *Journal of Medical Entomology* **52**, 1203–1212
969 (2015).
- 970 44. Tsunoda, T. *et al.* Winter Refuge for *Aedes aegypti* and *Ae. albopictus* Mosquitoes in Hanoi during Winter.
971 *PLOS ONE* **9**, e95606 (2014).
- 972 45. World Bank Data: Air transport, passengers carried - Vietnam. *World Bank*
973 <https://data.worldbank.org/indicator/IS.AIR.PSGR?locations=VN>.

- 974 46. *Water supply and sanitation in Vietnam: turning finance into services for the future*. (2014).
- 975 47. Tuyet Hanh, T. T. *et al.* Vietnam Climate Change and Health Vulnerability and Adaptation Assessment, 2018.
- 976 *Environ Health Insights* **14**, 1178630220924658 (2020).
- 977 48. Liu, X. *et al.* High-spatiotemporal-resolution mapping of global urban change from 1985 to 2015. *Nat Sustain*
- 978 **3**, 564–570 (2020).
- 979 49. Muñoz-Sabater, J. *et al.* ERA5-Land: a state-of-the-art global reanalysis dataset for land applications. *Earth*
- 980 *System Science Data* **13**, 4349–4383 (2021).
- 981 50. Cucchi, M. *et al.* WFDE5: bias-adjusted ERA5 reanalysis data for impact studies. *Earth Syst. Sci. Data* **12**,
- 982 2097–2120 (2020).
- 983 51. Beguería, S. & Vicente-Serrano, S. SPEI: Calculation of the Standardised Precipitation-Evapotranspiration
- 984 Index. R package v 1.7. (2017).
- 985 52. Beguería, S., Vicente-Serrano, S. M., Reig, F. & Latorre, B. Standardized precipitation evapotranspiration index
- 986 (SPEI) revisited: parameter fitting, evapotranspiration models, tools, datasets and drought monitoring.
- 987 *International Journal of Climatology* **34**, 3001–3023 (2014).
- 988 53. Vicente-Serrano, S. M., Beguería, S. & López-Moreno, J. I. A Multiscalar Drought Index Sensitive to Global
- 989 Warming: The Standardized Precipitation Evapotranspiration Index. *Journal of Climate* **23**, 1696–1718 (2010).
- 990 54. *General Statistics Office of Vietnam data source: passengers carried by road by province (last accessed January*
- 991 *2022)*.
- 992 55. An intuitive Bayesian spatial model for disease mapping that accounts for scaling - Andrea Riebler, Sigrunn H
- 993 Sørbye, Daniel Simpson, Håvard Rue, 2016.
- 994 [https://journals.sagepub.com/doi/10.1177/0962280216660421?url_ver=Z39.88-](https://journals.sagepub.com/doi/10.1177/0962280216660421?url_ver=Z39.88-2003&rfr_id=ori:rid:crossref.org&rfr_dat=cr_pub%20%20pubmed)
- 995 [2003&rfr_id=ori:rid:crossref.org&rfr_dat=cr_pub%20%20pubmed](https://journals.sagepub.com/doi/10.1177/0962280216660421?url_ver=Z39.88-2003&rfr_id=ori:rid:crossref.org&rfr_dat=cr_pub%20%20pubmed).
- 996 56. Hofman, J. M. *et al.* Integrating explanation and prediction in computational social science. *Nature* 1–8 (2021)
- 997 doi:10.1038/s41586-021-03659-0.
- 998 57. Hofman, J. M., Sharma, A. & Watts, D. J. Prediction and explanation in social systems. *Science* (2017)
- 999 doi:10.1126/science.aal3856.
- 1000 58. Bell, B. *et al.* The ERA5 global reanalysis: Preliminary extension to 1950. *Quarterly Journal of the Royal*
- 1001 *Meteorological Society* **147**, 4186–4227 (2021).
- 1002 59. Tran, H. P. *et al.* Householder perspectives and preferences on water storage and use, with reference to
- 1003 dengue, in the Mekong Delta, southern Vietnam. *International Health* **2**, 136–142 (2010).
- 1004 60. Pham, H. V., Doan, H. T., Phan, T. T. & Tran Minh, N. N. Ecological factors associated with dengue fever in a
- 1005 central highlands Province, Vietnam. *BMC Infectious Diseases* **11**, 172 (2011).

- 1006 61. Toan, D. T. T., Hoat, L. N., Hu, W., Wright, P. & Martens, P. Risk factors associated with an outbreak of dengue
1007 fever/dengue haemorrhagic fever in Hanoi, Vietnam. *Epidemiol. Infect.* **143**, 1594–1598 (2015).
- 1008 62. Schmidt, W.-P. *et al.* Population Density, Water Supply, and the Risk of Dengue Fever in Vietnam: Cohort Study
1009 and Spatial Analysis. *PLoS Med* **8**, e1001082 (2011).
- 1010 63. Akanda, A. S. & Johnson, K. Growing water insecurity and dengue burden in the Americas. *The Lancet*
1011 *Planetary Health* **2**, e190–e191 (2018).
- 1012 64. Mudau, N. & Mhangara, P. Towards understanding informal settlement growth patterns: Contribution to SDG
1013 reporting and spatial planning. *Remote Sensing Applications: Society and Environment* **27**, 100801 (2022).
- 1014 65. O'Reilly, K. M. *et al.* Projecting the end of the Zika virus epidemic in Latin America: a modelling analysis. *BMC*
1015 *Medicine* **16**, 180 (2018).
- 1016 66. Grubaugh, N. D. *et al.* Genomic epidemiology reveals multiple introductions of Zika virus into the United
1017 States. *Nature* **546**, 401–405 (2017).
- 1018 67. Alcayna, T. *et al.* Climate-sensitive disease outbreaks in the aftermath of extreme climatic events: A scoping
1019 review. *One Earth* **5**, 336–350 (2022).
- 1020 68. Padmanabha, H., Soto, E., Mosquera, M., Lord, C. C. & Lounibos, L. P. Ecological Links Between Water Storage
1021 Behaviors and *Aedes aegypti* Production: Implications for Dengue Vector Control in Variable Climates.
1022 *EcoHealth* **7**, 78–90 (2010).
- 1023 69. Tran, H. P. *et al.* Low Entomological Impact of New Water Supply Infrastructure in Southern Vietnam, with
1024 Reference to Dengue Vectors. *The American Journal of Tropical Medicine and Hygiene* **87**, 631–639 (2012).
- 1025 70. Colón-González, F. J. *et al.* Limiting global-mean temperature increase to 1.5–2 °C could reduce the incidence
1026 and spatial spread of dengue fever in Latin America. *Proceedings of the National Academy of Sciences* **115**,
1027 6243–6248 (2018).
- 1028 71. Ebi, K. Using Detection And Attribution To Quantify How Climate Change Is Affecting Health. *Health Affairs* **39**,
1029 2168–2174 (2020).
- 1030 72. United Nations. *Ready for the Dry Years: Building Resilience to Drought in South-East Asia*. (UN, 2019).
1031 doi:10.18356/adcaf1d0-en.
- 1032 73. Zhang, L., Chen, Z. & Zhou, T. Human Influence on the Increasing Drought Risk Over Southeast Asian
1033 Monsoon Region. *Geophysical Research Letters* **48**, e2021GL093777 (2021).
- 1034 74. Nguyen, C. T. *et al.* Prevalence of Zika virus neutralizing antibodies in healthy adults in Vietnam during and
1035 after the Zika virus epidemic season: a longitudinal population-based survey. *BMC Infectious Diseases* **20**, 332
1036 (2020).

- 1037 75. Quan, T. M. *et al.* Evidence of previous but not current transmission of chikungunya virus in southern and
1038 central Vietnam: Results from a systematic review and a seroprevalence study in four locations. *PLoS Negl*
1039 *Trop Dis* **12**, e0006246 (2018).
- 1040 76. Pebesma, E. Simple Features for R: Standardized Support for Spatial Vector Data. *The R Journal* **10**, 439
1041 (2018).
- 1042 77. Baston, D. exactextractr: Fast Extraction from Raster Datasets using Polygons. R package v 0.7.2. (2021).
- 1043 78. Hijmans, R. raster: Geographic Data Analysis and Modeling. R package version 3.5-2. (2021).
- 1044 79. Simini, F., González, M. C., Maritan, A. & Barabási, A.-L. A universal model for mobility and migration patterns.
1045 *Nature* **484**, 96–100 (2012).
- 1046 80. Hersbach, H. *et al.* The ERA5 global reanalysis. *Q.J.R. Meteorol. Soc.* **146**, 1999–2049 (2020).
- 1047 81. Mistry, M. N. *et al.* Comparison of weather station and climate reanalysis data for modelling temperature-
1048 related mortality. *Sci Rep* **12**, 5178 (2022).
- 1049 82. Bakka, H. *et al.* Spatial modeling with R-INLA: A review. *WIREs Computational Statistics* **10**, e1443 (2018).
- 1050 83. Rue, H. *et al.* Bayesian Computing with INLA: A Review. *Annu. Rev. Stat. Appl.* **4**, 395–421 (2017).
- 1051 84. Roberts, D. R. *et al.* Cross-validation strategies for data with temporal, spatial, hierarchical, or phylogenetic
1052 structure. *Ecography* **40**, 913–929 (2017).
- 1053